phys. stat. sol. (b) **245**, No. 10, 2319–2322 (2008) / **DOI** 10.1002/pssb.200879632

physica status solidi b
www.pss-b.com
basic solid state physics

Soliton fiber laser mode-locked by a single-wall carbon nanotube-polymer composite

F. Wang, A. G. Rozhin, Z. Sun, V. Scardaci, I. H. White, and A. C. Ferrari*

Department of Engineering, University of Cambridge, 9 JJ Thomson Avenue, Cambridge, CB3 0FA, UK

Received 2 May 2008, revised 24 June 2008, accepted 25 June 2008
Published online 29 August 2008

PACS 42.55.Wd, 42.65.Re, 78.67.Ch, 81.07.Pr

* Corresponding author: e-mail acf26@cam.ac.uk, Phone: +44-1223-748351, Fax: +44-1223-748348

We present a detailed investigation of pulse width and spectral dynamics of an Er^{3+}-doped soliton fiber ring laser, mode-locked by a carbon-nanotube-polymer composite. The laser is stable and produces $\sim$ 650 fs pulses at a fundamental repetition rate of 20.8 MHz. The carbon nanotube saturable absorber has a low saturation intensity of $\sim$ 18.9 MW/cm^2 and a 16.9% reduction in absorption (due to saturation) at high pulse intensity ($\sim$ 270 MW/cm^2). Spectral and transient effects confirm the soliton operation of the laser.

1 Introduction Single-wall carbon nanotubes (SWNTs) have attracted much attention in the field of optical communications in recent years, due to their ultrafast nonlinear optical properties in the near IR arising from saturation of excitonic transitions [1, 2, 4, 5]. Their potential applications include all-optical switching, passive mode-locking, and noise suppression for long-haul transmission systems. Following the first report of mode-locking [5], extensive research has focused on SWNTs mode-locking applications and has since led to a number of demonstrations [6–18]. Up to now, a fast recovery time on the scale of 500 fs has been confirmed both for SWNTs-polyimide composites [1] and for SWNT thin-films [16]. A high optical damage threshold (>2 mJ/cm^2) was also reported for SWNT thin-films [16]. In addition, SWNT based saturable absorbers have advantages such as wide absorption bandwidth from 1 to 2 μm and potential to integrate with micro-chip lasers due to small footprint and simplified device preparation compared with semiconductor saturable absorber mirrors (SESAMs) [19]. To date, fiber lasers [6–13], waveguide lasers [14] and solid-state lasers [15, 16] have been successfully mode-locked using SWNTs or SWNTs-polymer composites. Recent developments include mode-locking a Fabry-Pérot cavity based on a semiconductor optical amplifier at a fundamental repetition rate of 17.2 GHz [17], and the use of vertically aligned SWNT films interacting with the evanescent optical field inside a D-shaped fiber [18]. Although the number of reports of SWNT mode-locked lasers is increasing and the minimum achievable pulse duration has gone below 200 fs [10, 20], there has been no detailed discussion on the dynamics of such lasers. This has limited the understanding of the underlying mode-locking mechanisms and prevented clear design guidelines for such devices.

Here, we present the dynamics of a mode-locked Er^{3+} fiber laser, which employs a SWNTs-polyvinyl alcohol (PVA) composite as the mode-locking element. The laser produces ~650 fs soliton pulses at a repetition rate of 20.8 MHz. Detailed spectral and transient dynamics are recorded at different pumping levels and the operation of the laser is linked to the characteristics of the SWNTs-PVA saturable absorber. Spectral sidebands and low-intensity background in the output pulses confirm the soliton operation.

2 Experimental setup SWNTs are prepared by laser ablation [21]. The growth conditions are carefully adjusted so that the SWNTs have maximum absorption around ~1550 nm to coincide with the desired operating wavelength of the laser [9]. The composite preparation was described in Ref. [9]. Figure 1(a) shows the absorption spectra of our sample. The device is formed by sandwiching a SWNTs-PVA film between two fibre ferrules inside a physical contact ferrule connector (FC/PC) [9].

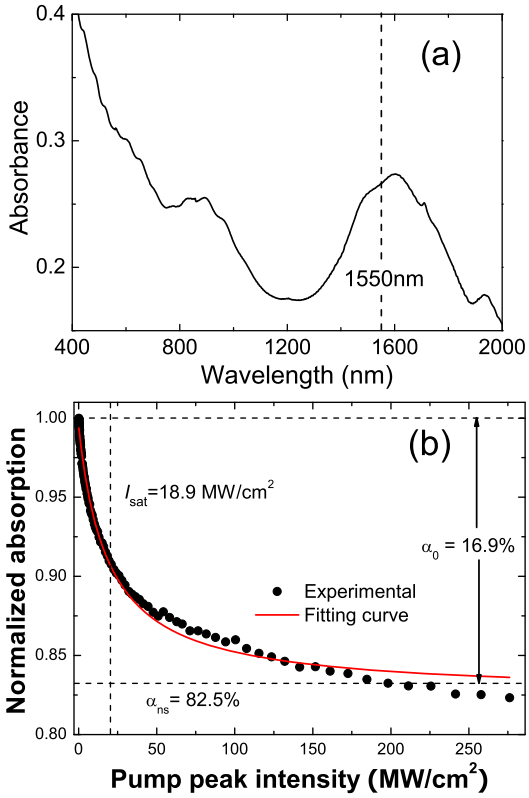

Figure 1 (a) Absorption spectrum of SWNTs-PVA composite film. (b) Normalized nonlinear power-dependent absorbance measurements using 650 fs pulses at 1550 nm.

The saturable absorption is characterized using 650 fs pump pulses at 1550 nm from a commercial femtosecond fiber laser (Toptica Photonics, AG) operating at 76 MHz. Figure 1(b) shows the power dependent absorbance measurements. We fit the experimental data according to a simple saturable absorber model [23]

$$\alpha(I) = \frac{\alpha_0}{1 + I/I_{sat}} + \alpha_{ns} \qquad (1)$$

where α_0 is the linear limit of the saturable absorption component, α_{ns} is the non-saturable absorption component and I_{sat} is the saturation intensity [23]. This reveals a saturable absorption of 16.9% and a saturation intensity of$\sim$18.9 MW/cm^2. Repeated measurements after two hours irradiation at high intensity ($\sim$270 MW/cm^2) show no significant degradation of the composite, indicating good thermal stability. The relatively large non-saturable absorbance of 82.5% is assigned to both the film non-saturated absorbance and the linear divergence loss at the fibre mode coupler, due to the film thickness [9].

Figure 2 illustrates the laser setup. A 1 m highly-doped Er^{3+} fiber (EDF) acts as the gain medium. It is pumped by a 980nm laser diode (LD) via a wavelength division multiplexer (WDM). Two isolators (ISO) are placed at both

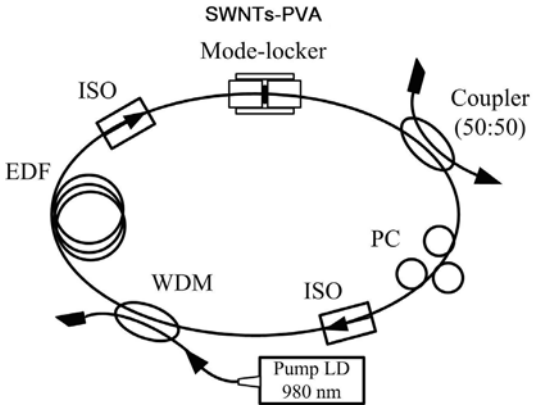

Figure 2 Laser Setup. (EDF: Er^{3+}-doped fiber, ISO: isolator, WDM: wavelength division multiplexer, PC: polarization controller, LD: laser diode).

ends of the Er^{3+} fiber to maintain unidirectional operation. The mode-locker immediately follows the isolator at the exit of the amplification section and light is coupled out of the cavity via a 50/50 coupler. A polarization controller (PC) is used to optimize the mode-locking condition. The total length of the laser cavity L is estimated to be 9.66 meters with mean cavity dispersion $\overline{\beta} = -27.5$ ps^2/km.

3 Results and discussion At low pump powers, the laser operates in an unstable Q-switched state. At 40 mW stable mode-locking self-starts. The laser can mode-lock at three discrete wavelengths: 1547, 1549, 1554 nm. These can be selected by changing the settings of the polarization controller, 1554 nm being the most stable against polarization perturbations. Such wavelength tuning in passively mode-locked fiber ring lasers was observed before in non-nanotube systems, and is usually attributed to birefringence in the fiber ring cavity [24]. When pump power increases beyond 60mW, the laser starts operating in a multi-pulse mode. However, stable mode-locking can be achieved as soon as the pump power is brought back below 60 mW. Figure 3 shows the output AC traces and optical spectra recorded (after 2 m fiber pigtail) at different pump powers. The output pulse duration decreases with increasing pump power and a minimum value of $\sim$640 fs is obtained at a pump power of 58.2 mW. We also detect a growing low-intensity background (continuum) as the cavity power increases. This indicates increased strength of the dispersive waves when the soliton pulse adapts itself to the increased gain inside the laser cavity and may account for the destabilization of the soliton pulses [25]. The $\sim$ 30 dB peak to background ratio (10^3 contrast) is limited by the dynamic range of our autocorrelator and the relatively low input power. From Fig. 3(b), asymmetric spectral broadening is observed and this is caused by the sharp decrease of gain profile of the Er^{3+} fiber beyond 1560 nm. Five pairs of sidebands are also visible on both sides of the central

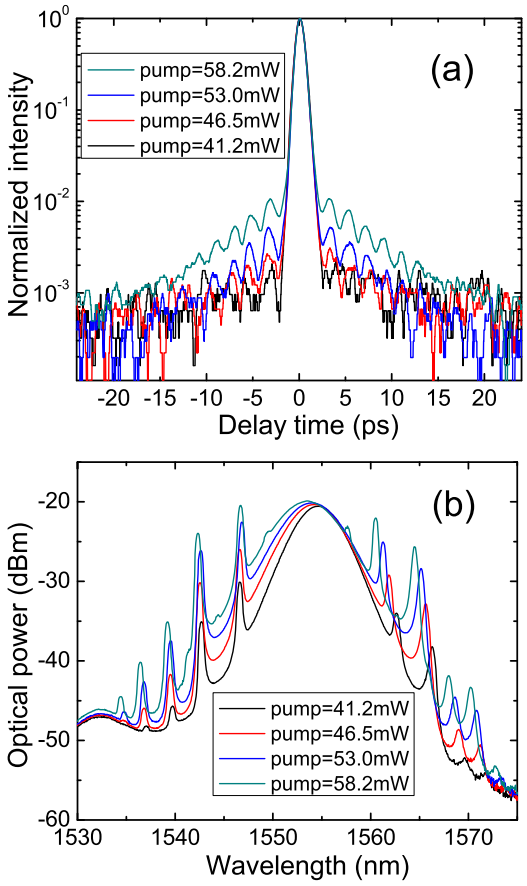

Figure 3 (a) Output autocorrelation traces. (b) Output spectra at four different pump levels. Bottom to top: increasing pump power 41.2; 46.5; 53; 58.2 mW.

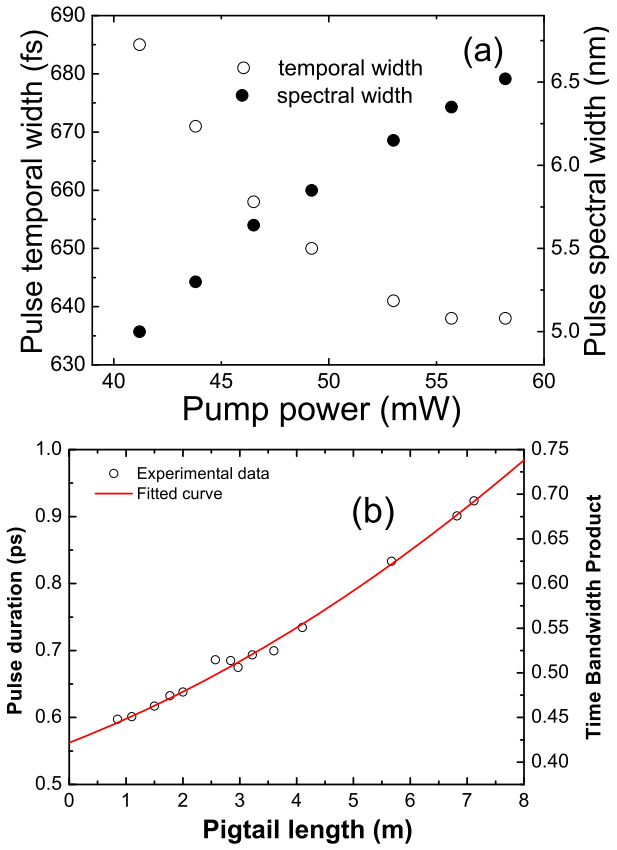

Figure 4 (a) Pulse spectral and temporal width as a function of pump power. (b) Pulse duration and time-bandwidth-product as a function of pigtail length.

wavelength. Their position agrees well with the prediction of sideband offsets of Ref. [26] and is typically due to periodic perturbations of the soliton fiber laser cavity [26]. When the pump power reaches 58.2 mW, fine structures appear between spectral peaks (Fig. 3(b)) and subsequent increase of pumping destroys the mode-locking. Fig. 4(a) shows the pulse spectral and temporal width as a function of pump power. The increase of the pulse spectral width is due to the enhanced self-phase-modulation within the cavity and confirms soliton formation [27]. The time bandwidth product corresponding to the shortest pulse width is 0.52, larger than the transform-limited prediction 0.315 for $Sech^2$ temporal profiles. Fibre lead cutback measurements shown in Fig. 4(b) give a time bandwidth product of 0.42 at the output of the laser, which is still slightly chirped. This residual chirp is believed to be caused by the soliton sideband generation and can be eliminated by suppressing the sidebands intensity [28, 29]. These results confirm the soliton operation of our laser.

The power incident onto our SWNTs-PVA film is 3.2-5.5 mW, corresponding to a peak intensity of 450-780 MW/cm^2, which is more than twenty times the saturation intensity of the mode-locker($\sim$18.9 MW/cm^2), indicating a full saturation regime. Figure 5(a) plots the RF spectrum of the first harmonic of the output. A 60 dB peak to background ratio (10^6 contrast) is observed at a resolution bandwidth of 9 kHz, located at $\sim$20.8 MHz, i.e. our fundamental cavity frequency. A slope efficiency of 4.25% can be derived from Fig. 5(b). Single pulse operation is also confirmed using an Agilent Infiniium Digital Communication Analyzer.

4 Conclusions We presented a detailed dynamics investigation of an ultrafast fiber laser mode-locked by a SWNTs-PVA film. Soliton pulse dynamics due to periodic perturbation of laser cavity are confirmed both by output spectra and autocorrelation traces. The laser produces $\sim$650 fs pulses at a repetition rate of 20.8 MHz. Optimized dispersion compensation of the cavity can be used to bring the pulse width further down.

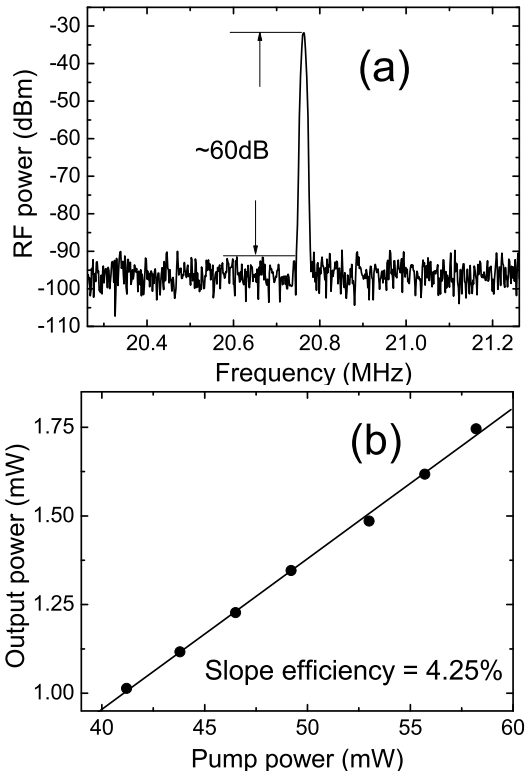

Figure 5 (a) RF power spectrum. (b) Output power as a function of pump power (fit gives slope efficiency = 4.25%).

Acknowledgements We thank F. Hennrich for providing laser ablation nanotubes. We acknowledge funding from Advance Nanotech Inc., EPSRC grants GR/S97613/01, EP/E500935/1, ETRI Ministry of Information and Communication, Republic of Korea, No. A1100-0602-0101, the Leverhulme Trust, the Isaac Newton trust and The Royal Society-Brian Mercer Innovation Award.

References

[1] Y.-C. Chen, N. R. Raravikar, L. S. Schadler, P. M. Ajayan,Y.-P. Zhao, T.-M. Lu, G.-C. Wang, and X.-C. Zhang, Appl. Phys. Lett. **81**, 975 (2002).

[2] T. Hertel, R. Fasel, and G. Moos, Appl. Phys. A **75**, 449 (2002).

[3] S. Tatsuura, M. Furuki, Y. Sato, I. Iwasa, M. Tian, and H. Mitsu, Adv. Mater. **15**, 534 (2003).

[4] J.-S. Lauret, C. Voisin, G. Cassabois, C. Delalande, P. Roussignol, O. Jost, and L. Capes, Phys. Rev. Lett. **90**, 057404 (2003).

[5] S. Y. Set, H. Yaguchi, Y. Tanaka, M. Jablonski, Y. Sakakibara, A. Rozhin, M. Tokumoto, H. Kataura, Y. Achiba, and K. Kikuchi, OSA Trends in Optics and Photonics (TOPS), Optical Fiber Communication Conference (OFC), Technical Digest, Postconference edition, Vol. 86 (Optical Society of America, Washington DC, 2003), p. 44.

[6] S. Y. Set, H. Yaguchi, Y. Tanaka, and M. Jablonski, J. Lightwave Technol. **22**, 51 (2004).

[7] S. Y. Set, H. Yaguchi, Y. Tanaka, and M. Jablonski, IEEE J. Sel. Top. Quantum Electron. **10**, 137 (2004).

[8] C. S. Goh, K. Kikuchi, S. Y. Set, D. Tanaka, T. Kotake, M. Jablonski, S. Yamashita, and T. Kobayashi, in: Conference on Lasers and Electro-Optics (CLEO) (Optical Society of America, 2005), paper CThG2.

[9] A. G. Rozhin, V. Scardaci, F. Wang, F. Hennrich, I. H. White, W. I. Milne, and A. C. Ferrari, phys. stat. sol. (b) **243**, 3551 (2006).

[10] A. G. Rozhin, Y. Sakakibara, S. Namiki, M. Tokumoto, H. Kataura, and Y. Achiba, Appl. Phys. Lett. **88**, 51118 (2006).

[11] Y.-W. Song, S. Yamashita, and S. Maruyama, Appl. Phys. Lett. **92**, 021115 (2008).

[12] V. Scardaci, A. G. Rozhin, F. Hennrich, W. I. Milne, and A. C. Ferrari, Physica E **37**, 115 (2007).

[13] V. Scardaci, A. G. Rozhin, P. Tan, F. Wang, I. H. White, W. I. Milne,and A. C. Ferrari, phys. stat. sol. (b) **244**, 4303(2007).

[14] G. D. Valle, R. Osellame, G. Galzerano, N. Chiodo,G. Cerullo, P. Laporta, O. Svelto, U. Morgner, A. G. Rozhin,V. Scardaci, and A. C. Ferrari, Appl. Phys. Lett. **89**, 231115 (2006).

[15] T. R. Schibli, K. Minoshima, H. Kataura, E. Itoga, N. Minami, S. Kazaoui, K. Miyashita, M. Tokumoto, and Y. Sakakibara, Opt. Express **13**, 8025 (2005).

[16] K. H. Fong, K. Kikuchi, C. S. Goh, S. Y. Set, R. Grange, M. Haiml, A. Schlatter, and U. Keller, Opt. Lett. **32**, 38 (2007).

[17] Y.-W. Song, S. Yamashita, C. S. Goh, and S. Y. Set, Opt. Lett. **32**, 430 (2007).

[18] Y.-W. Song,S. Yamashita, E. Einarsson, and S. Maruyama, Opt. Lett. **32**, 1399 (2007).

[19] O. Okhotnikov, A. Grudinin, and M. Pessa, New J. Phys. **6**, 177 (2004).

[20] M. Nakazawa, S. Nakahara, T. Hirooka, M. Yoshida, T. Kaino, and K. Komatsu, Opt. Lett. **31**, 915 (2006).

[21] S. Lebedkin, P. Schweiss, B. Renker, S. Malik, F. Hennrich, M. Neumaier, C. Stoermer, and M. M. Kappes, Carbon **40**, 417 (2002).

[22] H. Kataura, Y. Kumazawa, Y. Maniwa, I. Umezu, S. Suzuki, Y. Ohtsuka, and Y. Achiba, Synth. Met. **103**, 2555 (1999).

[23] E. Garmire, IEEE J. Sel. Top. Quantum Electron. **6**, 1094 (2000).

[24] W. S. Man, H. Y. Tam, M. S. Demokan, P. K. A. Wai, and D. Y. Tang, J. Opt. Soc. Am. B **17**, 28 (2000).

[25] J. P. Gordon, J. Opt. Soc. Am. B **9**, 91 (1992).

[26] M. L. Dennis and I. N. Duling, IEEE J. Quantum Electron. **30**, 1469 (1994).

[27] G. P. Agrawal, Nonlinear Fiber Optics, 3rd ed. (Academic Press, 2001).

[28] L. E. Nelson, D. J. Jones, K. Tamura, H. A. Haus, and E. P. Ippen, Appl. Phys. B **65**, 277 (1997).

[29] K. Tamura, E. P. Ippen, and H. A. Haus, IEEE Photonics Technol. Lett. **6**, 1433 (1994).

